

Aeroelastic analysis of a slender bridge deck based on a Computational Fluid Dynamics algorithm

A.V. Lopes

Faculty of Sciences and Technology, University of Coimbra, Portugal, avlopes@dec.uc.pt

Álvaro Cunha

Faculty of Engineering, University of Porto, Portugal, acunha@fe.up.pt

L.M.C. Simões

Faculty of Sciences and Technology, University of Coimbra, Portugal, lcsimoes@dec.uc.pt

ABSTRACT: This paper presents a new methodology for the aeroelastic analysis of slender structures, based on the appropriate conjugation of an algorithm of Computational Fluid Dynamics (Finite Volume Method) with algorithms for either linear or geometrically non-linear analysis of structures. The computer code developed on the basis of this methodology was applied to the aeroelastic study of a simply supported slender bridge deck, with rectangular cross-section. Some of the most meaningful results associated with the analysis of the corresponding aeroelastic instability are presented.

1 INTRODUCTION

Wind action is one of the most determining factors for the safety of large and flexible structures. As it is well known, since the famous Tacoma Narrows Bridge failure of 1940, the design of long span cable-stayed and suspension bridges requires careful study of their aeroelastic behaviour under wind loads.

Traditionally, this kind of work has been based on physical models tested in wind tunnels. More recently, an alternative numerical approach has been developed and refined. This empirical theory, based on the so-called Scanlan model for the evaluation of the wind forces (aeroelastic forces), involves important simplifications, which depend on the aeroelastic phenomena to be considered. However, this analytical approach requires the identification of some coefficients (drag, lift, moment coefficients and flutter derivatives). They are usually obtained from experimental studies on sectional bridge models in wind tunnels, though recent developments of Computational Fluid Dynamics (CFD) allow an alternative numerical approach.

In this context, the main objective of this paper is to present a new methodology for the integral aeroelastic analysis of slender structures, based on the appropriate conjugation of an algorithm of Computational Fluid Dynamics (Finite Volume Method) with an algorithm of linear or geometrically non-linear analysis of structures. The computer code developed on the basis of this new methodology was applied to the aeroelastic study of a simply supported slender bridge deck, with rectangular cross-section.

2 INTEGRAL AEROELASTIC ANALYSIS

The computational algorithm developed to simulate aeroelastic phenomena in slender structures is a time incremental approach based on two numerical algorithms working together: one of them determining the fluid flow action and the other one evaluating the structural response. The numerical procedure used to calculate the fluid flow and its action on structures is based on the Finite Volume Method. The Finite Element Method is used to model the structural dynamic behaviour, which can be idealised as geometrically non-linear.

2.1 Fluid flow simulation

The program, based on the Finite Volume Method (Patankar 1980, Versteeg 1995, Ferziger 1996), is suitable to simulate incompressible and isotherm bidimensional unsteady fluid flows around obstacles. It is assumed that the flow domain may be discretised in a control volume mesh, whose faces have vertical and horizontal directions. Differential forms of the general transport equations are discretised using a hybrid differentiation scheme. To reduce false diffusion, the quick differentiation scheme is also used in deferred correction context. Alternate value fields are avoided on the basis of a staggered grid approach. Solution procedures for transient calculations are implemented adapting under-relaxation factors depending on time increment. The high Reynolds number $k - \epsilon$ turbulence model is applied to simulate the flow turbulence (Rodi 1980, Tennekes 1980, Hossain 1982 and Oliveira 1990).

The iterative solution procedures for every time increment are the *TDMA* line-by-line solver of the governing mass, momentum and turbulence conservation algebraic equations of unsteady turbulent flow, and the *SIMPLE* algorithm to ensure correct linkage between pressure and velocity.

The convergence criterion for pressure-correction equations is set up by

$$\frac{1}{n} \sum_n \frac{\|{}^i b\|}{\rho U} \leq 10^{-4} \quad (1)$$

where n is the number of control volumes, ${}^i b$ is the source term at the i^{th} iteration, ρ is the fluid density and U is the flow velocity out of domain.

For the remaining equations, the convergence criterion is given by

$$\frac{1}{n} \sum_n \frac{\|{}^i \phi - {}^{i-1} \phi\|}{\phi_{inlet}} \leq 10^{-4} \quad (2)$$

where ${}^i \phi$ is the field value calculated at the i^{th} iteration and ϕ_{inlet} is the field value in the inlet domain.

2.2 Structural analysis

The Finite Element Method is used to model the structural behaviour (Bathe 1982, Zienkiewicz 1989, Clough 1993). The simulation of the dynamic behaviour is based on incremental Newmark Method and the corresponding integration parameters are set up according to Newmark initial proposal (constant-average-acceleration-method). Structural damping is introduced assuming a Rayleigh damping matrix, where the mass and stiffness matrix coefficients are evaluated by adopting the two first modal damping factors.

The numerical procedures, based on an Updated Lagrangian formulation, permit the domain of global large displacements consideration (geometrical non-linear behaviour). The convergence criterion for non-balanced forces is

$$\frac{1}{n} \sum_n \frac{\|{}^i a - {}^{i-1} a\|}{L_{ref}} \leq 10^{-6} \quad (3)$$

where n is the number of degrees of freedom, ${}^i a$ is the displacement value calculated at the i^{th} iteration and L_{ref} is a reference dimension.

Small element deformations were adopted to evaluate the structural response.

2.3 Aeroelastic algorithm

A structural system is submitted to several forces when immersed in a fluid flow (Simiu 1986 and Naudasher 1994). They depend on three fundamental effects:

- External flow instability, by velocity field fluctuations in external domain;
- Internal flow instability, by structural geometry and flow characteristics;
- Structural movements.

When the structural movements play an important role in terms of force characteristics the correspondent forces are named self-excited. If the structure is flexible, these forces have a significant influence on the structural movements. The forces associated to the structure-flow interaction are called aeroelastic forces, and they depend, not only on the flow characteristics around the structural system, but also on the structural flexibility.

Therefore, the numerical algorithm to simulate aeroelastic phenomena in an incremental form must consider this correspondence between aeroelastic forces and structural movements at every time step (Lopes 2001). It should be considered that in any new time step, the values of both aeroelastic forces and structural movements are unknown. However, it is possible to use an iterative subprocess to achieve the convergence at the end of the time step. When compared with incremental structural analysis, the time interval used in normal fluid flow simulations is very short. In such case, the rates of forces change are higher than those of movement changes. In order to consider the structural inertia, it is possible to have a very good prediction about the movements at the end of each time step, by using linear extrapolation such as

$${}^{t+\Delta t} \ddot{a}_k = 2 {}^t \ddot{a}_k - {}^{t-\Delta t} \ddot{a}_k \quad (4)$$

It's worth noting that only structural transversal velocities and rotations are important to be quantified in the fluid flow simulation context. So, by using the Newmark Method formulation, it is possible to obtain velocity and displacement predictions.

The iterative subprocess associated to each time increment begins based on those predictions. Then the algorithm solves the flow equations and calculates the aeroelastic forces. Now, it is possible to determine the corresponding structural movements. If those movements are not in good agreement with the predictions, these predictions must be corrected and this subprocess is reinitiated until convergence is achieved. Due to the characteristics of bidimensional fluid flow simulation, this algorithm considers several transversal cross sections along the slender part of the structure where the aeroelastic forces are calculated. This simplified procedure assumes that the flow is normal to the longitudinal axis of the slender structure. Moreover the flow around one section may be simulated by itself and is independent from the other sections. Due to computational limitations, it is only possible to simulate the flow in a reduced number of sections.

2.4 Simulation of structural movements in fluid flow

Consider a free obstacle imerse in a bidimensional fluid flow, with the corresponding movements being characterized by displacement functions a_{ij} in agreement with Ox_{ij} axis directions.

These movements can be modeled indirectly by changing the velocity components (v_1 and v_2) of fluid flow at external inlet boundary domain. For example, one obstacle translation a_i , in correspondence with Ox_i axis, can be modeled by specifying the velocity components of fluid flow at an inlet boundary domain through

$$v_j \rightarrow v_j - \dot{a}_i \delta_{ij} \quad (5)$$

where \dot{a}_i is the velocity of the obstacle translation.

On the other hand, one obstacle rotation a_{12} , in correspondence with Ox_{12} axis, can be modeled by specifying the velocity components of fluid flow at inlet boundary domain through

$$\begin{bmatrix} v_1 \\ v_2 \end{bmatrix} \rightarrow T \cdot \begin{bmatrix} v_1 \\ v_2 \end{bmatrix} \quad (6)$$

where T is the transformation matrix

$$T = \begin{bmatrix} \cos a_{12} & \sin a_{12} \\ -\sin a_{12} & \cos a_{12} \end{bmatrix} \quad (7)$$

In this previous case, the aeroelastic forces have to be determined according to Ox_{ij} axes, which represent general directions for structural analysis and for drag, lift and moment aeroelastic forces. This can be done by modifying the aeroelastic forces obtained while using the transformation

$$\begin{bmatrix} F_1 \\ F_2 \end{bmatrix} \leftarrow T^T \cdot \begin{bmatrix} F_1 \\ F_2 \end{bmatrix} \quad (8)$$

3 NUMERICAL SIMULATION OF AEROELASTIC INSTABILITY

This new methodology was applied to the aeroelastic analysis of a simply supported slender bridge deck, with rectangular cross-section (Fig. 1). This structure was modeled with 10 beam elements, with the same length, whose mechanical characteristics are presented in Table 1. Table 2 shows the first nine natural frequencies and respective mode types. Structural damping was idealized on the basis of a Rayleigh damping matrix, whose composition was determined assuming modal damping factors of 0.5% for the first vertical bending and torsional modes. The evaluation of the aeroelastic forces was made by simulating the fluid flow around sections 3, 6 and 9. The fluid flow mesh was built using 88x53 control volumes (with a minimum dimension of

5E-2m and a maximum of 77E-2m). The air at standard conditions was the fluid considered.

The simulations consider four different flow velocities (70, 75, 80 and 85m/s). Before releasing the structure, the simulation assumed that the fluid flow leads to a stable condition with oscillatory characteristics considering each velocity flow. Figures 3-22 present some more significant results concerning displacements and aeroelastic forces at the midspan section.

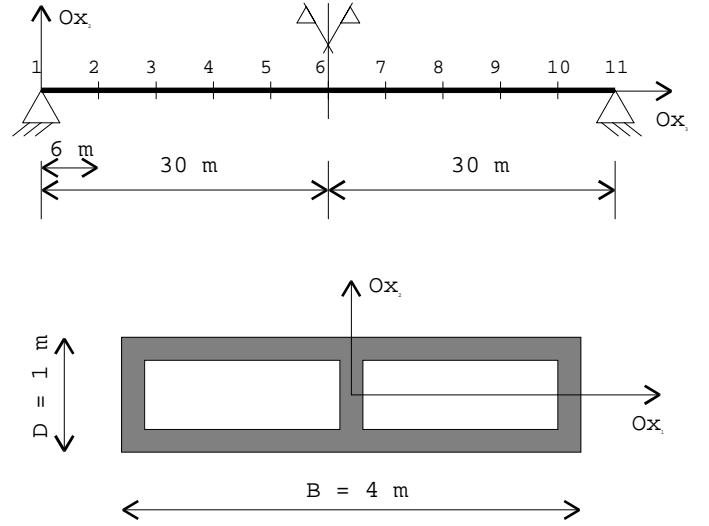


Figure 1. Geometry of simply supported slender bridge deck.

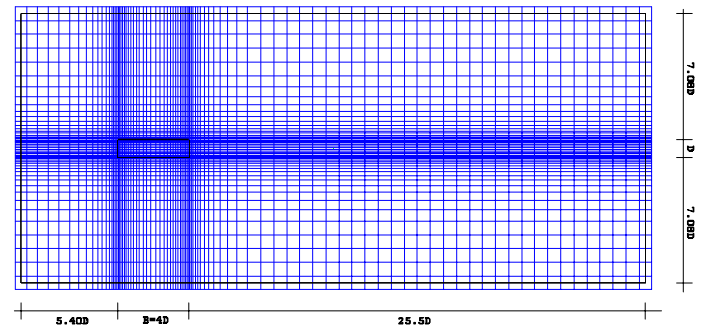


Figure 2. Control volume mesh for fluid flow simulation.

Table 1. Characteristics of beam elements.

Axial stiffness (EA)	3E7 kN
Ox_1 flexural stiffness (EI_1)	6E6 kN.m ²
Ox_2 flexural stiffness (EI_2)	6E7 kN.m ²
Torsional stiffness (GI_p)	1E6 kN.m ²

Table 2. Natural frequencies.

Mode n°	Mode type	Frequency (Hz)
1	1st vertical	0.68
2	1st horizontal	2.14
3	2nd vertical	2.70
4	1st torsional	3.57
5	3rd vertical	6.09
6	2nd torsional	7.22
7	2nd horizontal	8.55
8	4th vertical	10.33
9	3rd torsional	11.06

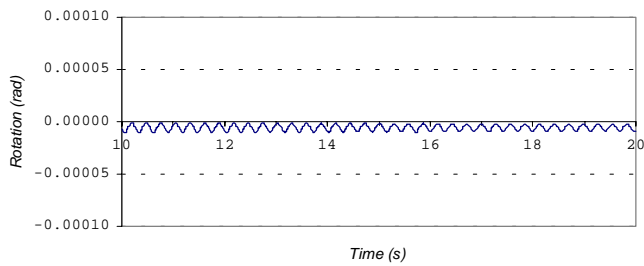


Figure 3. Rotation at midspan section. Flow velocity: 70m/s. Interval 10-20s.

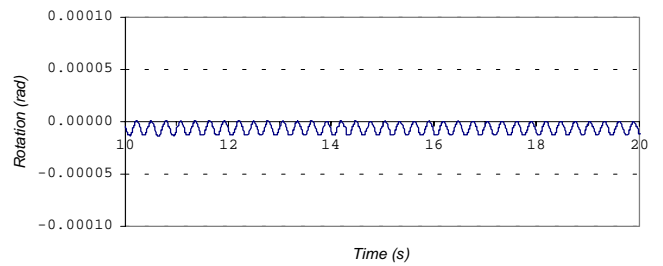


Figure 8. Rotation at midspan section. Flow velocity: 75m/s. Interval 10-20s.

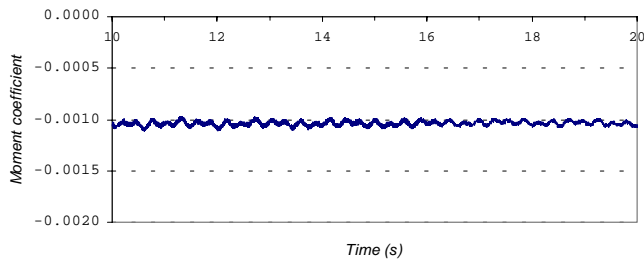


Figure 4. Moment coefficient at midspan section. Flow velocity: 70m/s. Interval 10-20s.

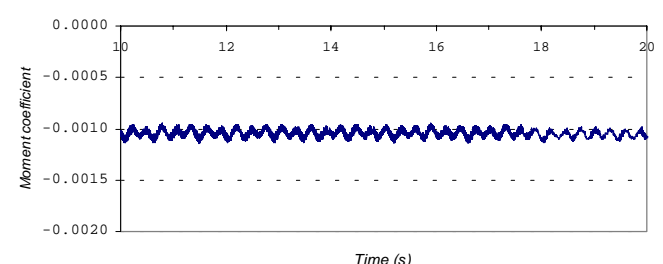


Figure 9. Moment coefficient at midspan section. Flow velocity: 75m/s. Interval 10-20s.

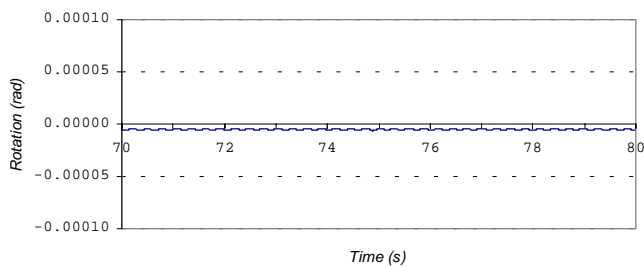


Figure 5. Rotation at midspan section. Flow velocity: 70m/s. Interval 70-80s.

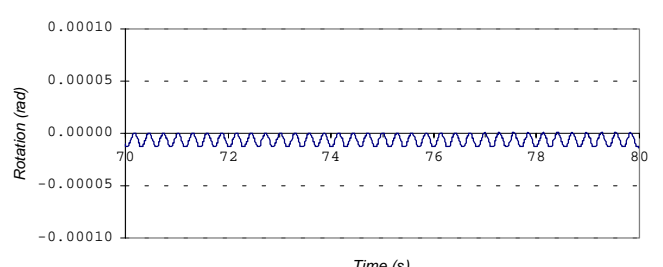


Figure 10. Rotation at midspan section. Flow velocity: 75m/s. Interval 70-80 seconds.

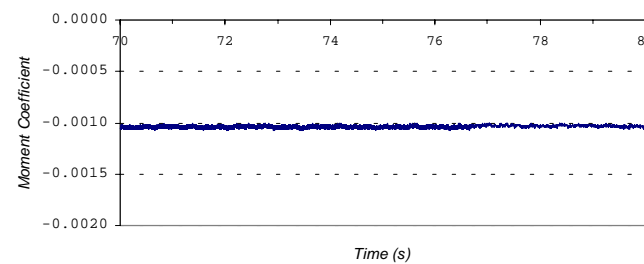


Figure 6. Moment coefficient at midspan section. Flow velocity: 70m/s. Interval 70-80s.

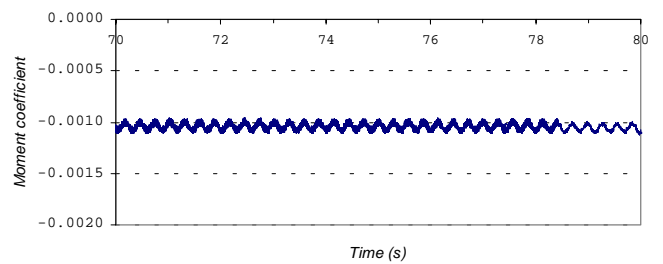


Figure 11. Moment coefficient at midspan section. Flow velocity: 75m/s. Interval 70-80s.

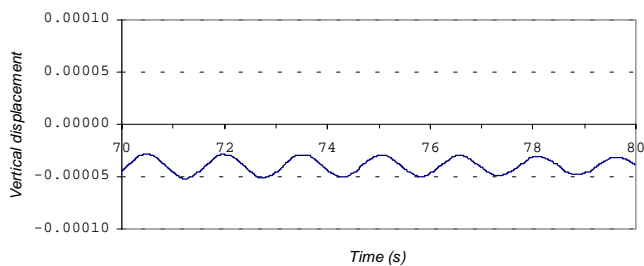


Figure 7. Vertical displacement at midspan section. Flow velocity: 70m/s. Interval 70-80s

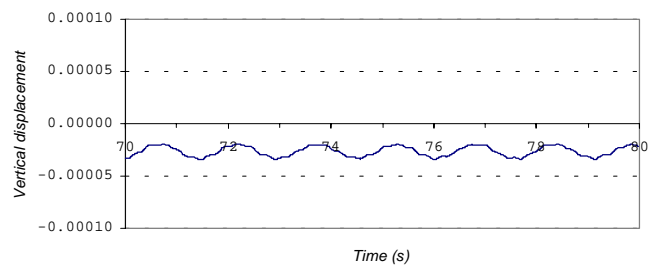


Figure 12. Vertical displacement at midspan section. Flow velocity: 75m/s. Interval 70-80s.

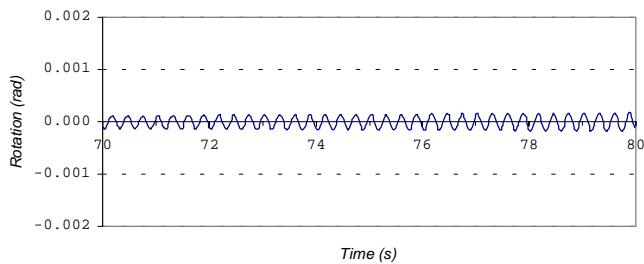


Figure 13. Rotation at midspan section. Fluid flow: 80m/s. Interval 70-80s.

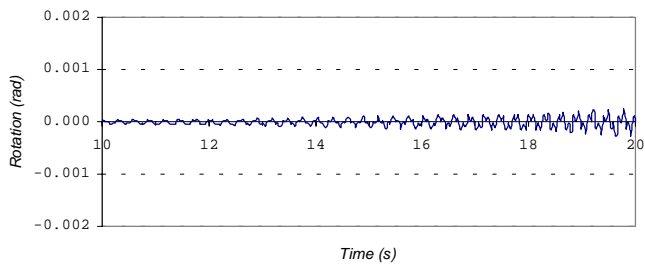


Figure 18. Rotation at midspan section. Fluid flow: 85m/s. Interval 10-20s.

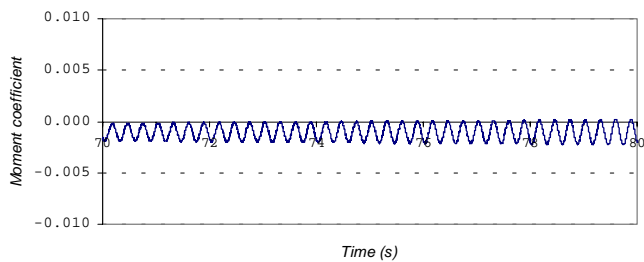


Figure 14. Moment coefficient at midspan section. Fluid flow: 80m/s. Interval 70-80s.

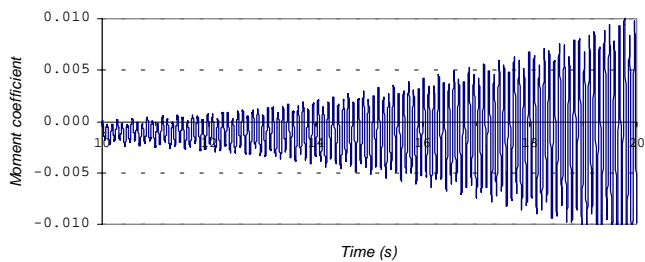


Figure 19. Moment coefficient at midspan section. Fluid flow : 85m/s. Interval 10-20s.

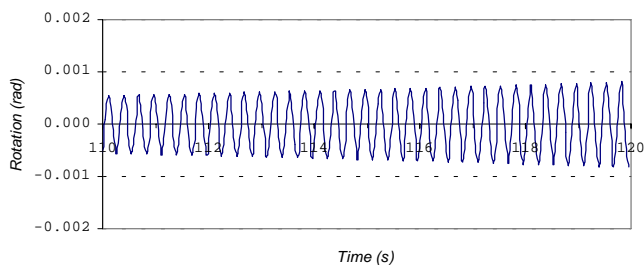


Figure 15. Rotation at midspan section. Fluid flow: 80m/s. Interval 110-120s.

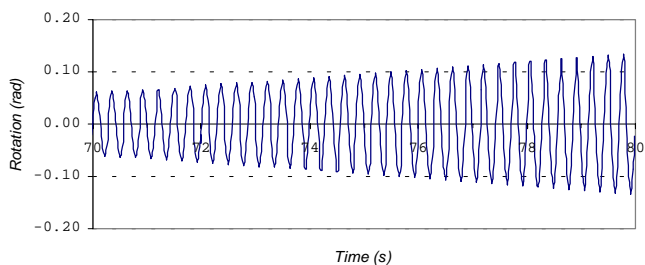


Figure 20. Rotation at midspan section. Fluid flow: 85m/s. Interval 70-80s.

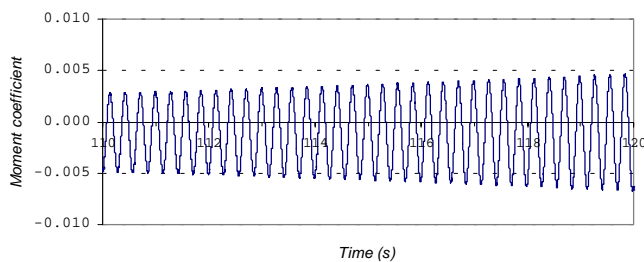


Figure 16. Moment coefficient at midspan section. Fluid flow : 80m/s. Interval 110-120s.

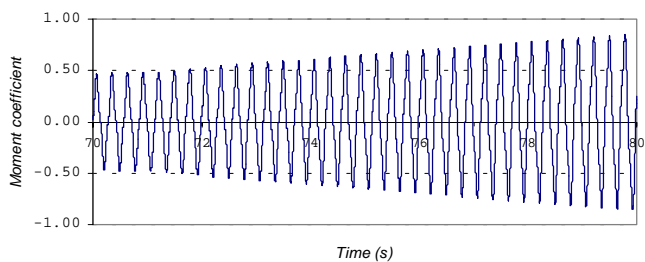


Figure 21. Moment coefficient at midspan section. Fluid flow: 85m/s. Interval 70-80s.

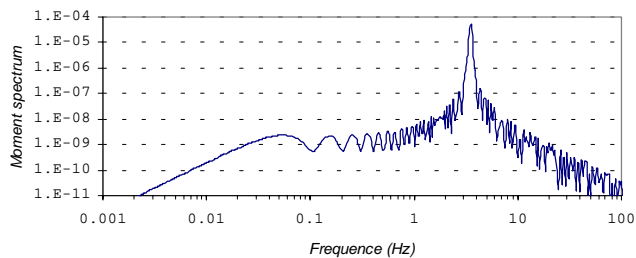


Figure 17. Moment spectrum at midspan section. Fluid flow: 80m/s. Interval 110-120s.

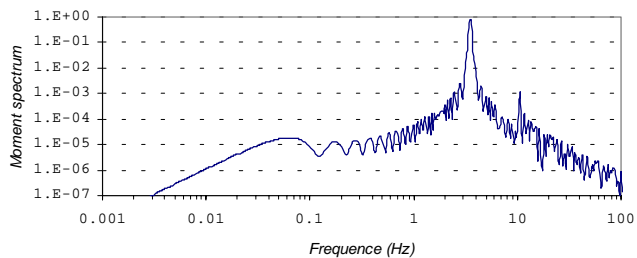


Figure 22. Moment spectrum at midspan section. Fluid flow: 85m/s. Interval 70-80s.

Inspection of these results permit to draw the following particular conclusions:

- The structure will not become unstable for a flow velocity of 70m/s, because the amplitude of rotations, as well as aeroelastic moments do not increase when compared to the response in the time intervals 70-80s and 10-20s;
- The structure may eventually become unstable for a flow velocity of 75m/s, after a long time, as the amplitude of rotations show some incipient increase in the interval 70-80s with regard to 10-20s;
- The structure will become unstable for a flow velocity of 80m/s, because undergoes a clear increase of rotations in the time interval 110-120s. Beyond that, the amplitude of the aeroelastic moments increase continuously in that same period of time, showing an oscillatory dominant frequency coincident with the frequency of rotations;
- After a short period of time the structure will become unstable for a flow velocity of 85m/s, as the amplitude of rotations increases much faster from the period 10-20s to 70-80s. In this case, the amplitude of aeroelastic moments quickly increases in the interval 10-20s, whereas the aeroelastic moments show a continuous growing in the period 70-80s, and also an oscillatory dominant frequency coincident with the frequency of rotations. Moreover, the amplitude of aeroelastic moments grows much faster than rotations when compared with the simulation for a flow velocity of 80m/s.

4 CONCLUSIONS

The results presented here illustrate a new numerical methodology for the integral aeroelastic analysis of slender structures, based on the appropriate conjugation of an algorithm of Computational Fluid Dynamics (Finite Volume Method) with an algorithm for the geometrically non-linear analysis of structures.

The computer code developed on the basis of this new methodology was applied to the aeroelastic study of a simply supported slender bridge deck, with rectangular cross-section, which enabled the characterisation of possible forms of aeroelastic instability for different flow velocities.

Further research will be now carried out to more complex structures, particularly to long span bridges, and the results can be confronted with existing data.

5 REFERENCES

- Bathe, Klaus-Jürgen; 1982; Finite Element Procedures in Engineering Analysis; Prentice-Hall, New Jersey.
- Clough, R. W. & Penzien, J.; 1993; Dynamics of Structures; McGraw-Hill.
- Ferziger, J. H. & Peric, M.; 1996; Computational Methods for Fluid Dynamics; Springer-Verlag Berlin Heidelberg.
- Hossain, M. S. & Rodi, W.; 1982; A turbulence Model for Buoyant Flows and its application to Vertical Buoyant Jets; Turbulent Buoyant Jets and Plumes; Pergamon Press; Oxford; p. 121-178.
- Lopes, A. V.; 2001; Aplicação da Dinâmica Computacional de Fluidos à Análise Aeroelástica de Estruturas Esbeltas; Ph.D. Tesis; Departamento de Eng. Civil; FCTUC; Coimbra; Portugal.
- Naudascher, E. & Rockwell, D.; 1994; Flow-Induced Vibrations: An engineering guide; A. A. Balkema, Rotterdam, Netherlands.
- Oliveira, L. A.; 1990; Modelação Numérica de Escoamentos em Regime Turbulento; Departamento de Eng. Mecânica; Faculdade de Ciências e Tecnologia da Universidade de Coimbra.
- Patankar, S. V.; 1980; Numerical Heat Transfer and Fluid Flow; Hemisphere Publishing Corporation.
- Rodi, W.; 1980; Turbulence Models and Their Application in Hydraulics – A State of the Art Review; International Association for Hydraulic Research; Delft, Netherlands.
- Simiu E. & Scanlan, R.; 1986; Wind effects on structures. An introduction to wind engineering; John Wiley & Sons.
- Tennekes, H. & Lumley, J. L.; 1980; A first Course in Turbulence; Sixth Printing; Massachusetts Institute of Technology Press; Massachusetts.
- Versteeg, H. K. & Malalasekera, W.; 1995; An Introduction to Computational Fluid Dynamics; Longman Malaysia.
- Zienkiewicz, O. C. & Taylor, R. L.; 1989; The Finite Element Method; Fourth edition; McGraw-Hill.